PERGAMON

International Journal of Solids and Structures 38 (2001) 2189–2202

INTERNATIONAL JOURNAL OF SOLIDS and STRUCTURES

www.elsevier.com/locate/ijsolstr

Effects of piezoactuator delamination on the transfer functions of vibration control systems

Andrzej Tylikowski *

Institute of Machine Des Fund, Warsaw University of Technology, Narbutta 84, 02-524 Warsaw, Poland

Received 7 August 1999; in revised form 19 December 1999

Abstract

The purpose of this theoretical work is to present a general bending–extensional model of the response of a simply supported laminated beam to excitation by a nonsymmetric actuator made using piezoelectric elements. The edge delamination is modeled by changing the effective length of debonded actuator. Dynamic equations, joint conditions between sections with and without active layers as well as the boundary conditions at the two ends of the beam form a boundary value problem. The dynamic strain response to the excitation by the applied voltage term is determined from the solution of this boundary value problem. The dynamic extensional strain on the beam surface is calculated by including the free stress conditions at the piezoelectric actuator boundaries, by considering the dynamic coupling between the actuator and the beam, and by taking into account a finite bonding layer with the finite stiffness. The analysis indicates that the edge delamination has a harmful effect on the performance of piezoactuators, but the significant decrease of natural frequencies with an increase in delamination length is not observed. The influence of the delamination length on the system transfer functions (the beam surface strain, the beam transverse displacement and the shear stresses in bonding layers) is shown.

Keywords: Vibration control; Piezoelectric actuators; Delaminations; Transfer functions

1. Introduction

Piezoelectric materials show great advantages as actuators in intelligent structures, i.e., structures with highly distributed actuators, sensors, and processor networks. Piezoelectric sensors and actuators have been applied successfully in the closed loop control (Bailey and Hubbard, 1985; Newman, 1991). The beam vibration due to the excitation of a piezoelectric actuator has been modeled by Crawley and de Luis (1987) and Jie Pan et al. (1991). In particular, Crawley and de Luis presented a comprehensive static model for a piezoelectric actuator glued to a beam. The relationship between static structural strains, both in the structure and in the actuator, and the applied voltage across the piezoelectric was presented. This static approach was then used to predict the dynamic behavior. As the shear modulus of bonding layers increases or the thickness of bonding layers decreases the shear lag becomes less significant and the shear stresses are

* Fax: +48-22-660-8622.
E-mail address: aty@simr.pw.edu.pl (A. Tylikowski).

0020-7683/01/$ - see front matter
PII: S0020-7683(00)00161-X

transferred from actuators to the beam over small regions close to the piezoelectric ends. For the perfectly bonding layers, the tangential stress distribution is described by the two Dirac-delta functions located at the piezoelement ends. High shear stresses can cause a crack initiation and propagations in bonding layer, delamination or even total debonding of piezoelectric element. A dynamic model for a simply supported beam with a piezoelectric actuator glued to each of its upper and lower surfaces was developed by Jie Pan et al. (1991). In their model, the actuators were assumed to be perfectly bonded. This means that the bonding layer is sufficiently thin so that the shear of layer can be neglected. The effect of through-width delamination on the vibration characteristics of laminated beams without piezoactuators was studied by Mujumdar and Suryanarayan (1988). The influence of composite plate delamination on buckling of the debonded layers was discussed by Jiang and Bao (1996). Analysis performed by Bogdanovich and Rastogi (1996) shows that complete and accurate solving of bonded plates can be only obtained in 3-D elasticity formulation and numerical solutions. Kim and Jones (1992) investigated the effect of delamination on the performance of piezoactuators which are surface mounted on a cantilever beam assuming a pure bending model and the mass per unit area of the piezoelement and the beam equal to one. They show that the edge delamination significantly decreases the coupling performance of piezoactuators.

In the present paper, a bending–extensional dynamic model of the beam-bonding layer-actuators system, is proposed. The pure extensional strain in the piezoelectric elements and the massless bonding layers are assumed. The dynamic extensional strain on the beam surface is calculated by including the free stress conditions at the piezoelectric actuator boundaries, by considering the dynamic coupling between the actuator and the beam, and by taking into account a finite bonding layer with the finite stiffness. The approach has been used (Tylikowski, 1993) to derive a control strategy especially useful in collocated sensor–actuator systems. The used dynamic equations can be reduced to the particular cases from past studies, which were based on the assumption of static coupling between the actuator and the beam or assuming the perfect bonding in dynamical analysis.

2. Analysis

Consider the elastic beam with the identical piezoelectric layers mounted on each of two opposite sides. Fig. 1 shows an edge delamination of the lower piezoactuator. For simplicity, it is also assumed that the gap width extends uniformly across the beam (Kim and Jones, 1992). The analysis will use the Bernoulli–Euler theory to describe a beam motion. The beam is assumed to be simply supported. Due to the geometry, the beam is divided into four parts as shown in Fig. 1, and the dynamic behavior of each part is described by different equations. The motion is described by the beam transverse displacement w due to bending and the pure longitudinal displacements u_{pe}^{+} and u_{pe}^{-} of upper and lower piezoelectric actuators, respectively. The

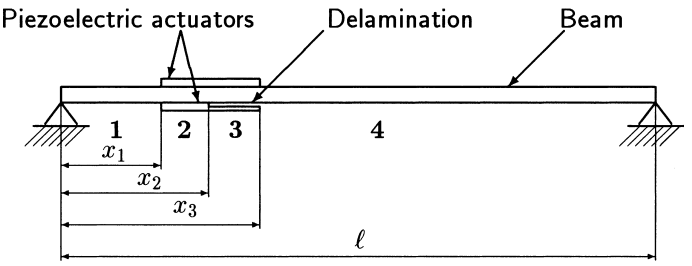

Fig. 1. Beam with partially debonded piezoelectric layers.

poling directions in both actuators are the same. The actuators are driven by a pair of electrical fields v with the same amplitude and in opposite phase.

The inertia forces of finite-thickness bonding layers are neglected and the pure one-dimensional shear in the bonding layer is assumed.

Consider an infinite element of beam and upper and lower actuators in the second section $x_1 < x < x_2$ shown in Fig. 2. The thickness of beam, bonding layer and piezoelectric actuator is denoted by t_b, t_s and t_{pe}, respectively.

The beam dynamics equations are as follows:

$$T_{,x} - \rho_b^* t_b b w_{,tt} = 0, \tag{1}$$

$$M_{,x} - T + b t_b(\tau^+ + \tau^-) = 0, \tag{2}$$

where $\rho_b^* = \rho_b(1 + 2(\rho_{pe} t_{pe}/\rho_b t_b))$ is the equivalent beam density, and the subscript comma denotes partial differentiation with respect to the variable after the comma.

Under the assumption of pure extensional strains in the piezoelectric elements their dynamic equations expressed by longitudinal strains $\epsilon^+ = u^+_{pe,x}$, $\epsilon^- = u^-_{pe,x}$ are

$$\rho_{pe} t_{pe} \epsilon^+_{,tt} - E_{pe} t_{pe} \epsilon^+_{,xx} + \tau^+_{,x} = 0, \tag{3}$$

$$\rho_{pe} t_{pe} \epsilon^-_{,tt} - E_{pe} t_{pe} \epsilon^-_{,xx} + \tau^-_{,x} = 0. \tag{4}$$

For the massless bonding layers, isotropic stress–strain relations are

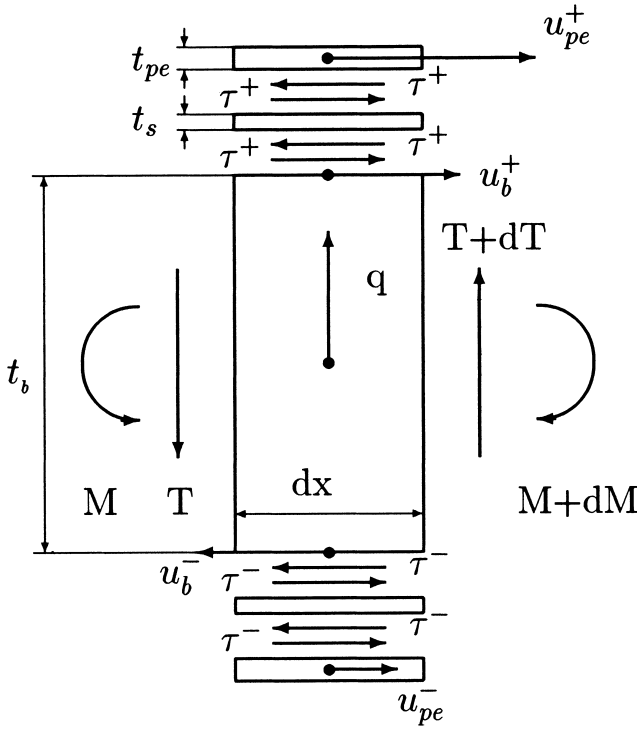

Fig. 2. Geometry of the beam in the second section.

$$\tau^+ = \frac{G}{t_s}(u^+_{pe} - u^+_b), \tag{5}$$

$$\tau^- = \frac{G}{t_s}(u^-_b - u^-_{pe}), \tag{6}$$

where E_b, is Young's modulus of beam, E_{pe}, Young's modulus of the piezoactuator, G, Kirchoff's modulus of bonding layer. The geometric relation on the beam surface leads to

$$w_{,xx} = -\frac{2}{t_b}u_{b,x} = -\frac{2}{t_b}\epsilon_b. \tag{7}$$

The bending moment M generated by the distributed normal stresses over the beam cross-section is equal to

$$M = \frac{t_b^2 b}{6}\sigma_b = \frac{E_b t_b^2 b}{6}\epsilon_b. \tag{8}$$

Eliminating displacements w, u^+_{pe}, u^-_{pe}, inner forces and shear stresses τ^+, τ^- we can write beam surface and piezoelectric strains dynamic equations (2) and (4) for Section 2 in the following form:

$$\rho_{pe}t_{pe}\epsilon^+_{,tt} - E_{pe}t_{pe}\epsilon^+_{,xx} + \frac{G}{t_s}(\epsilon^+ - \epsilon_b) = 0, \quad x \in (x_1, x_2), \tag{9}$$

$$\rho_{pe}t_{pe}\epsilon^+_{,tt} - E_{pe}t_{pe}\epsilon^+_{,xx} + \frac{G}{t_s}(\epsilon_b - \epsilon^-) = 0, \quad x \in (x_1, x_2), \tag{10}$$

$$\rho^*_b\epsilon_{b,tt} + \frac{E_b t_b^2}{12}\epsilon_{b,xxxx} + \frac{Gt_b}{4t_s}(\epsilon^+_{,xx} - \epsilon^-_{,xx} - 2\epsilon_{b,xx}) = 0, \quad x \in (x_1, x_2). \tag{11}$$

In the third section $x_2 < x < x_3$ shown in Fig. 3, the moment equation has a modified form due to the lack of shear between the beam and the lower actuator

$$M_{,x} - T + \frac{bt_b}{2}\tau^+ = 0. \tag{12}$$

Finally, we obtain two coupled partial differential equations in the third section of the form

$$\rho_{pe}t_{pe}\epsilon^+_{,tt} - E_{pe}t_{pe}\epsilon^+_{,xx} + \frac{G}{t_s}(\epsilon^+ - \epsilon_b) = 0, \quad x \in (x_2, x_3), \tag{13}$$

$$\rho^*_b\epsilon_{b,tt} + \frac{E_b t_b^2}{12}\epsilon_{b,xxxx} + \frac{Gt_b}{4t_s}(\epsilon^+_{,xx} - \epsilon_{b,xx}) = 0, \quad x \in (x_2, x_3). \tag{14}$$

The motion of the beam in the first and fourth sections is described by the classical Bernoulli–Euler equation, which can be obtained by neglecting the third term in Eq. (14).

$$\rho_b\epsilon_{b,tt} + \frac{t_b^2}{12}\epsilon_{b,xxxx} = 0, \quad x \in (0, x_1) \cup (x_3, \ell). \tag{15}$$

The stress–strain relationship for the piezoelectric material has the form

$$\sigma_{pe} = E_{pe}(u_{pe,x} - \Lambda), \tag{16}$$

where the piezoelectric strain, the piezoelectric constant, and the applied voltage are denoted by $\Lambda = d_{31}v/t_{pe}$, d_{31} and v, respectively.

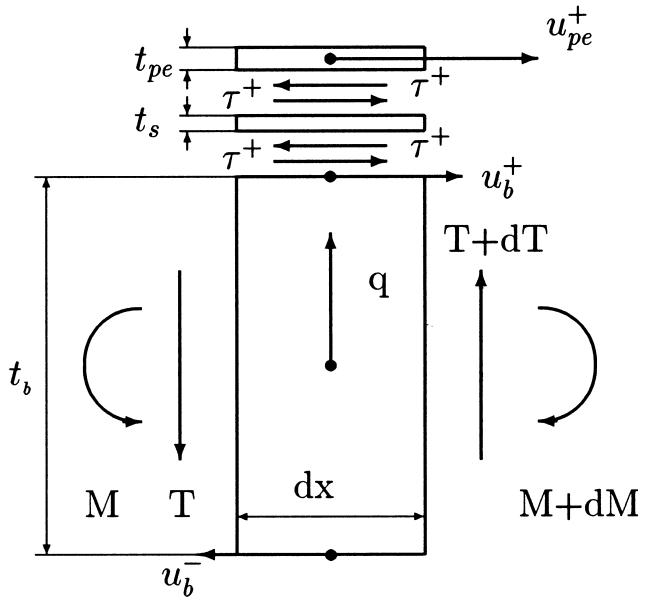

Fig. 3. Geometry of the beam in the third section (one-sided delamination region).

3. Boundary and joint conditions

We assume simply supported boundary conditions imposed on the solution of Eq. (15) at $x = 0$ and $x = \ell$, continuity of deflection, slope, curvature and transverse force for $x = x_1$, $x = x_2$ and $x = x_3$ as well as continuity of upper actuator displacement and upper actuator stress $x = x_2$. The continuity condition of transverse forces should take into account the presence of the shear stresses τ^+, τ^-, e.g. for $x = x_1$, we have

$$E_{\mathrm{b}} \frac{bt_{\mathrm{b}}^3}{12} w_{,xxx}(x_1^-) = E_{\mathrm{b}} \frac{bt_{\mathrm{b}}^3}{12} w_{,xxx}(x_1^+) - \frac{t_{\mathrm{b}} b}{2} (\tau^+(x_1^+) - \tau^-(x_1^+)) \tag{17}$$

and for $x = x_2$,

$$E_{\mathrm{b}} \frac{bt_{\mathrm{b}}^3}{12} w_{,xxx}(x_2^-) - \frac{t_{\mathrm{b}} b}{2} (\tau^+(x_2^-) - \tau^-(x_2^-)) = E_{\mathrm{b}} \frac{bt_{\mathrm{b}}^3}{12} w_{,xxx}(x_2^+) - \frac{t_{\mathrm{b}} b}{2} \tau^+(x_2^+). \tag{18}$$

Solutions should satisfy free edge conditions corresponding to the zero normal stresses at the ends of piezoactuators, which can be written in the form

$$\sigma_{\mathrm{pe}}^+(x_1^+) = \sigma_{\mathrm{pe}}^-(x_1^+) = \sigma_{\mathrm{pe}}^+(x_3^-) = \sigma_{\mathrm{pe}}^-(x_2^-) = 0. \tag{19}$$

Finally, full system of boundary and joint conditions have the form

$$w(0,t) = w(\ell,t) = 0, \tag{20}$$

$$w_{,xx}(0,t) = w_{,xx}(\ell,t) = 0, \tag{21}$$

$$w(x_1^-,t) = w(x_1^+,t), \quad w(x_2^-,t) = w(x_2^+,t), \quad w(x_3^-,t) = w(x_3^+,t), \tag{22}$$

$$w_{,x}(x_1^-,t) = w_{,x}(x_1^+,t), \quad w_{,x}(x_2^-,t) = w_{,x}(x_2^+,t), \quad w_{,x}(x_3^-,t) = w_{,x}(x_3^+,t), \tag{23}$$

$$w_{,xx}(x_1^-,t) = w_{,xx}(x_1^+,t), \quad w_{,xx}(x_2^-,t) = w_{,xx}(x_2^+,t), \quad w_{,xx}(x_3^-,t) = w_{,xx}(x_3^+,t), \tag{24}$$

$$T(x_1^-,t) = T(x_1^+,t), \quad T(x_2^-,t) = T(x_2^+,t), \quad T(x_3^-,t) = T(x_3^+,t), \tag{25}$$

$$\epsilon^+(x_1^+,t) = \epsilon^+(x_3^-,t) = \Lambda, \qquad \epsilon^-(x_1^+,t) = \epsilon^-(x_2^-) = -\Lambda, \tag{26}$$

$$u_{\mathrm{pe}}^+(x_2^-,t) = u_{\mathrm{pe}}^+(x_2^+,t), \qquad \epsilon^+(x_2^+,t) = (\epsilon_2^-,t). \tag{27}$$

4. Steady-state solution

Assuming a harmonic frequency excitation $\Lambda = \Lambda_0 \exp(\mathrm{i}\omega t)$ steady-state response of dynamic equations (9)–(11) and (13)–(15) are sought as harmonics with the same angular velocity

$$\begin{bmatrix} \epsilon^+(x,t) \\ \epsilon^-(x,t) \\ \epsilon_{\mathrm{b}}(x,t) \end{bmatrix} = \begin{bmatrix} \varepsilon^+(x) \\ \varepsilon^-(x) \\ \varepsilon_{\mathrm{b}}(x) \end{bmatrix} \exp(\mathrm{i}\omega t). \tag{28}$$

Substituting Eq. (28) into Eqs. (9)–(11) and (13)–(15), we obtain the system of ordinary differential equations solutions which have the form dependent on the section number.

Section 1

$$\varepsilon_{\mathrm{b}}(x) = C_1 \exp(k_1 x) + C_2 \exp(-k_1 x) + C_3 \exp(\mathrm{i}k_1 x) + C_4 \exp(-\mathrm{i}k_1 x), \tag{29}$$

where

$$k_1 = \sqrt[4]{\frac{12\rho_{\mathrm{b}}\omega^2}{E_{\mathrm{b}} t_{\mathrm{b}}^2}}.$$

Section 2

$$\varepsilon_{\mathrm{b}}(x) = \sum_{n=7}^{12} C_n \alpha(k_n,\omega) \exp(k_n x), \tag{30}$$

$$\varepsilon^+(x) = C_5 \exp(k_5 x) + C_6 \exp(-k_5 x) + \sum_{n=7}^{12} C_n \exp(k_n x), \tag{31}$$

$$\varepsilon^-(x) = C_5 \exp(k_5 x) + C_6 \exp(-k_5 x) - \sum_{n=7}^{12} C_n \exp(k_n x), \tag{32}$$

where

$$k_5 = \sqrt{\frac{G}{t_{\mathrm{s}} t_{\mathrm{pe}} E_{\mathrm{pe}}} - \frac{\rho_{\mathrm{pe}}}{E_{\mathrm{pe}}}\omega^2},$$

the wavenumbers k_i, $i = 7, \ldots, 12$ satisfy the following algebraic equation:

$$k^6\frac{E_b t_b^2}{12}E_{pe}t_{pe}+k^4\left[\rho_{pe}\frac{E_b t_b^2 t_{pe}}{12}\omega^2-\frac{Gt_b}{2t_s}\left(\frac{E_b t_b}{6}+E_{pe}t_{pe}\right)\right]-k^2\omega^2\left(\rho_{pe}\frac{t_{pe}t_b G}{2t_s}+\rho_b^* E_{pe}t_{pe}\right)$$
$$-\rho_b^*\omega^2\left(\rho_{pe}t_{pe}\omega^2-\frac{G}{t_s}\right)=0 \tag{33}$$

and

$$\alpha(k,\omega)=1-\frac{E_{pe}t_{pe}t_s}{G}k^2-\frac{\rho_{pe}t_{pe}t_s}{G}\omega^2.$$

Section 3

$$\varepsilon_b(x)=\sum_{n=13}^{18}C_n\alpha(k_n,\omega)\exp(k_n x), \tag{34}$$

$$\varepsilon^+(x)=\sum_{n=13}^{18}C_n\exp(k_n x), \tag{35}$$

where the wavenumbers k_i, $i=13,\ldots,18$ satisfy the following algebraic equation:

$$k^6\frac{E_b t_b^2}{12}E_{pe}t_{pe}+k^4\left[\rho_{pe}\frac{E_b t_b^2 t_{pe}}{12}\omega^2-\frac{Gt_b}{4t_s}\left(\frac{E_b t_b}{3}+E_{pe}t_{pe}\right)\right]-k^2\omega^2\left(\rho_{pe}\frac{t_{pe}t_b G}{4t_s}+\rho_b^* E_{pe}t_{pe}\right)$$
$$-\rho_b^*\omega^2\left(\rho_{pe}t_{pe}\omega^2-\frac{G}{t_s}\right)=0. \tag{36}$$

Section 4

$$\varepsilon_b(x)=C_{19}\exp(k_1 x)+C_{20}\exp(-k_1 x)+C_{21}\exp(ik_1 x)+C_{22}\exp(-ik_1 x). \tag{37}$$

The 22 unknown coefficients $C_1, C_2, \ldots, C_{22}$ are determined by the boundary and joint conditions described by Eqs. (20)–(27).

5. Results

Numerical calculations based on the formulae presented in the previous sections are performed for a wide range of angular frequency and $\Lambda = 0.0001$. More precisely, $\omega = 0.1$ s^{-1} for the static loading, in the first beam resonance region $\omega = 206$ s^{-1}, and for a high frequency $\omega = 1850$ s^{-1}. The dimensions of the steel beam are $l = 380$ mm, width $b = 40$ mm and thickness $t_b = 2$ mm. The piezoelectric actuators are located between $x_1 = 0.079$ m and $x_3 = 0.117$ m. The remaining dimensions are width $b = 40$ mm and thickness $t_{pe} = 0.6$ mm. The center of the piezoelectrics is located at $x = 98$ mm. The parameters of the beam and piezoelectric elements used in calculations are listed in Table 1. The mass per unit area ratio of the piezoelement and the beam is equal to 0.55. As there are no precise data available relating the Kirchhoff modulus G of bonding layer, and the bonding layer thickness t_s calculations are performed for the following values of parameter $G/t_s = 10^{10}, 10^{11}, 10^{12}$ corresponding to the soft, the intermediate and the stiff bonding, respectively. The main parameter is the relative length of delamination, where 0 corresponds to the no delamination. The dynamic characteristics are calculated for the four values of relative length of delamination of the lower actuator 0, 0.25, 0.5, and 0.75.

Figs. 4 and 5 show the beam responses to a cyclic piezoelectric strains applied to both piezoelectric actuators bonded to the beam in $x = 0.1$ m and $x = 0.34$ m, respectively. The magnitude of the transfer functions decreases as the delamination length increases. It is seen from details in Figs. 6 and 7 that the

Table 1
Material parameters used in calculations

Material	Beam–steel	Actuator–PZTG-1195
ρ (kg m^{-3})	7800	7275
E (N m^{-2})	21.6×10^{10}	63×10^{9}
t (m)	0.002	0.0006
d_{31} (m V^{-1})	–	1.9×10^{-10}

presence of delamination does not significantly decreases the first natural frequency. Figs. 8–10 show that the effect of delamination length does not change qualitatively the spatial distribution of beam displacement in the first resonance region as the bonding layer parameter G/t_s increases. It is observed that the del-

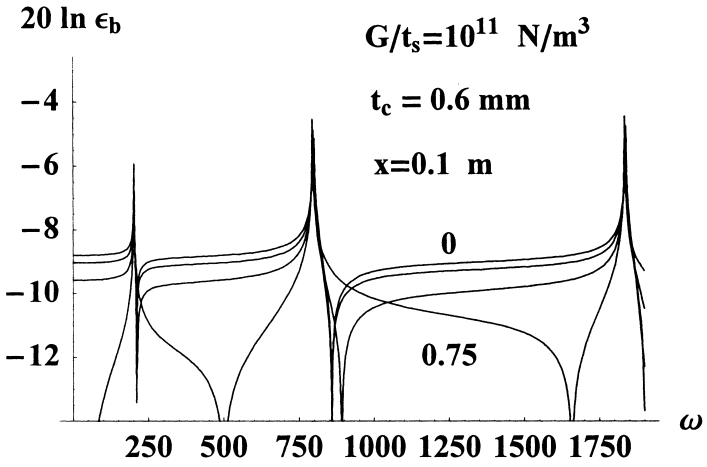

Fig. 4. Near field beam longitudinal response ϵ_b at $x = 0.1$ m.

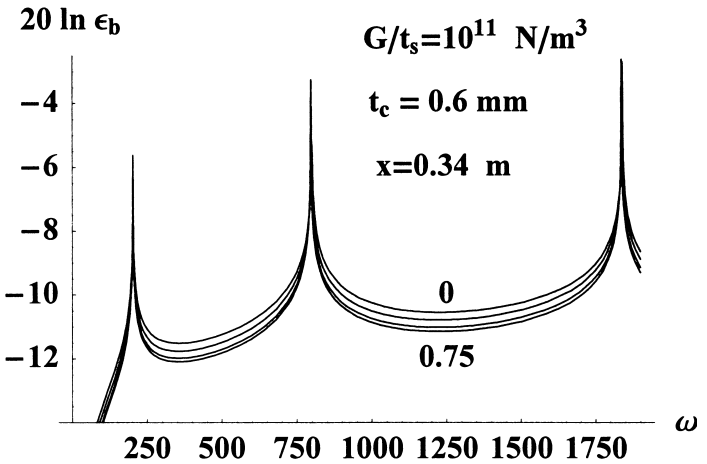

Fig. 5. Far field beam longitudinal response ϵ_b at $x = 0.34$ m.

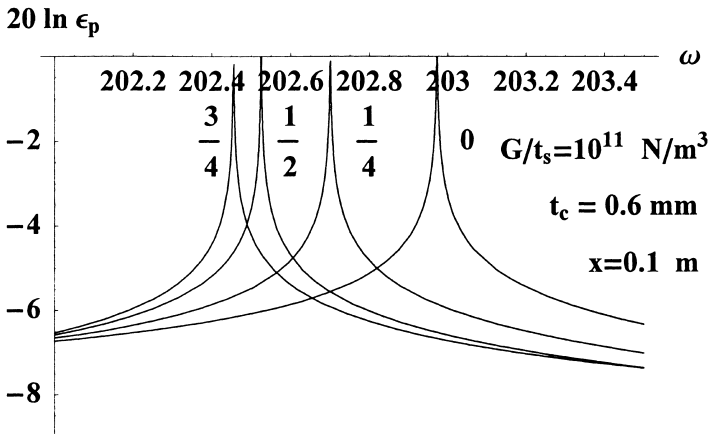

Fig. 6. Details of near field beam transverse response ϵ_b at $x = 0.1$ m in the first beam resonance.

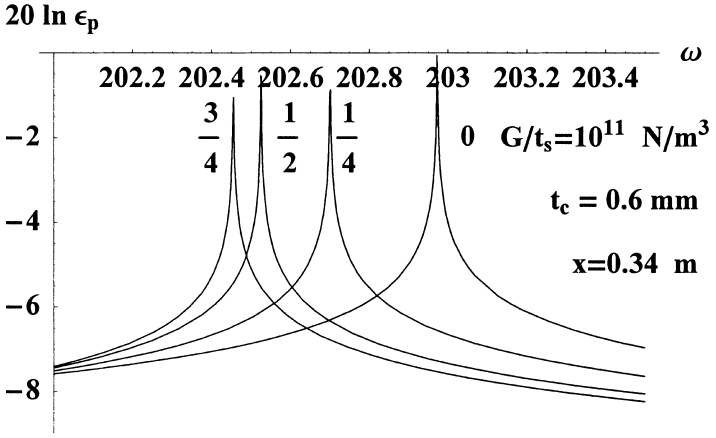

Fig. 7. Details of far field beam transverse response ϵ_b at $x = 0.34$ m in the first beam resonance.

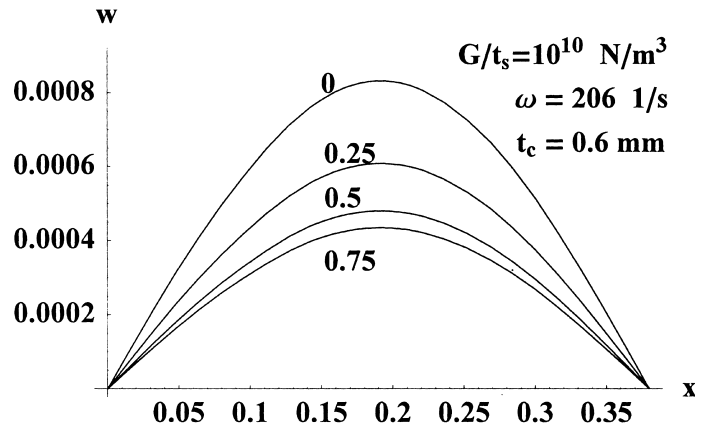

Fig. 8. Influence of relative delamination length on spatial beam displacement for soft bonding layer $G/t_s = 10^{10}$ N m^{-3}.

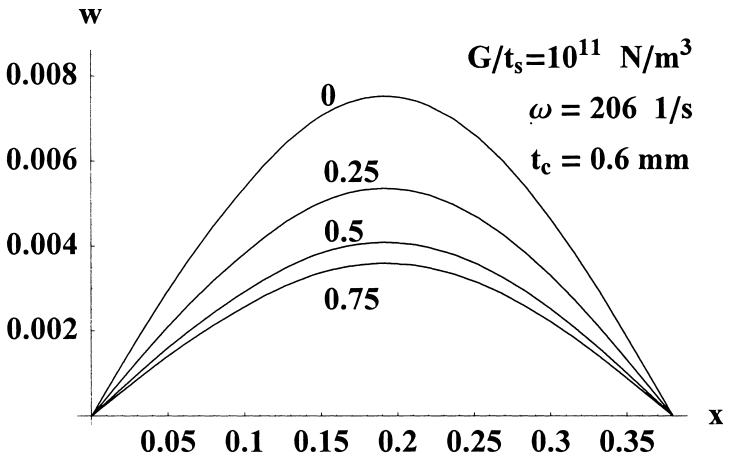

Fig. 9. Influence of relative delamination length on spatial beam displacement for intermediate bonding layer $G/t_s = 10^{11}\ \mathrm{N\,m^{-3}}$.

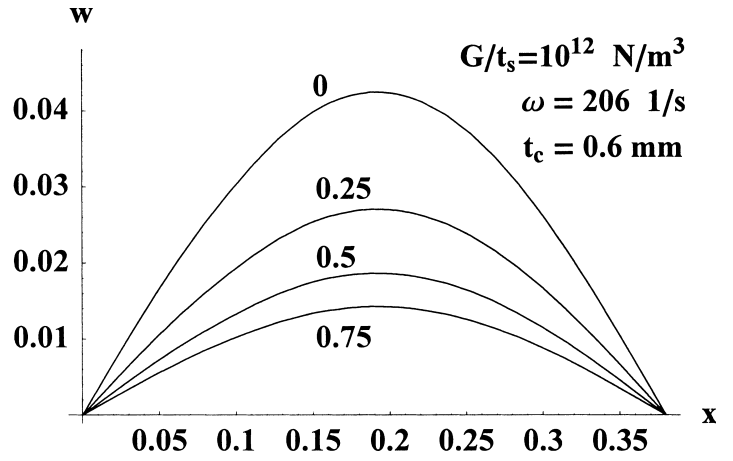

Fig. 10. Influence of relative delamination length on spatial beam displacement for stiff bonding layer $G/t_s = 10^{12}\ \mathrm{N\,m^{-3}}$.

amination decreases piezoactuator coupling performance independently of the bonding layer stiffness. It is seen that if the bonding layer parameter is increased the beam deflection increases. But the increase is more pronounced at small values of G/t_s. Comparison of Figs. 9, 11, and 12 show different spatial responses for different excitation frequencies. Fig. 11 shows the beam deflection at $\omega = 0.1\ \mathrm{s^{-1}}$ corresponding to a very slow excitation (static loading). As the inertia forces are negligible and there are no external forces in the first and fourth sections, the curvature is equal to zero and displacements are represented by straight lines. Due to the shear stresses in the second and the third section we have a curve with the nonzero curvature.

Integrating strains ε^+, ε^-, ε_b with respect to x and using formulae (5) and (6) yield the shear stresses in the bonding layers.

Section 2 $(x_1 < x < x_2)$

$$\tau^+ = \frac{G}{t_s}\left((C_5\exp(k_5x) - C_6\exp(-k_5x))/k_5 + \sum_{n=7}^{12}\frac{C_n}{k_n}(1-\alpha(k_n,\omega))\exp(k_nx)\right), \tag{38}$$

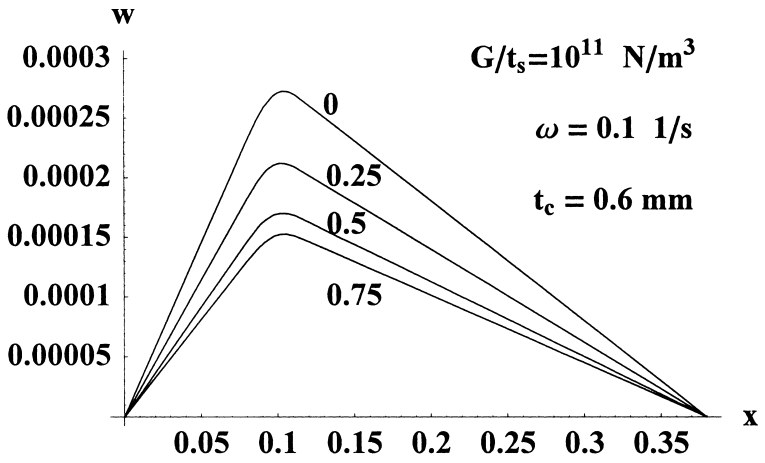

Fig. 11. Influence of relative delamination length on spatial beam displacement for quasistatic excitation $\omega = 0.1\ \mathrm{s}^{-1}$.

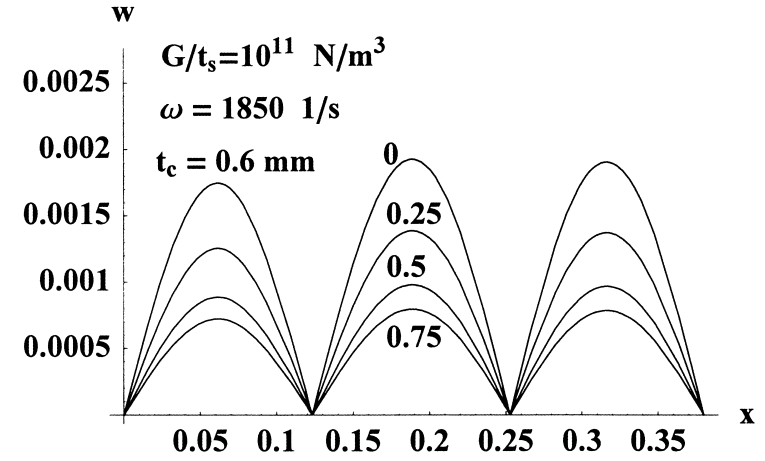

Fig. 12. Influence of relative delamination length on spatial beam displacement for high frequency excitation $\omega = 1850\ \mathrm{s}^{-1}$.

$$\tau^- = \frac{G}{t_s}\left((-C_5 \exp(k_5 x) + C_6 \exp(-k_5 x))/k_5 + \sum_{n=7}^{12} \frac{C_n}{k_n}(1 - \alpha(k_n, \omega)) \exp(k_n x) \right). \tag{39}$$

Section 3 $(x_2 < x < x_3)$

$$\tau^+ = \frac{G}{t_s} \sum_{n=13}^{18} \frac{C_n}{k_n}(1 - \alpha(k_n, \omega)) \exp(k_n, x), \tag{40}$$

$$\tau^- = 0. \tag{41}$$

Figs. 13 and 14 show the distributions of shear along the second and third sections as functions of x and the bonding layer parameter. The shear stress calculated according to present theory (Eqs. (30)–(41)) can be compared with the static shear stress for bonded piezoactuators without delamination (Crawley and de Luis, 1987) denoted by a dashed curve. The present dynamic analysis and the static one are in a qualitative

agreement. The shear stresses are antisymmetric with respect to the center of piezoelectric actuator. But the absolute values of the dynamic shear stresses are larger. For large G/t_s the stress distribution gathers in the regions close to the piezoactuator ends and converges to the distribution described by a linear form of the δ-Dirac functions concentrated at the piezoelement ends (Bailey and Hubbard, 1985). Comparison of the shear stresses for slowly varying excitations $\omega = 0.1\ s^{-1}$ calculated according to the present dynamical approach (continuous line) and the static model of Crawley and de Luis (1987) (dashed line) shows a good agreement (Fig. 15). The spatial dynamic stress distributions in the upper bonding layer and in the lower bonding layer are shown in Figs. 13 and 14, respectively. It is seen that the delamination qualitatively changes the stress distribution in the delamination region decreasing the performance of the lower piezoactuator. Despite the zero shear stresses in the third section of lower layer the increase of the shear stresses in the upper perfectly bonding layer is not observed. The presented results, however still wait for experimental verifications.

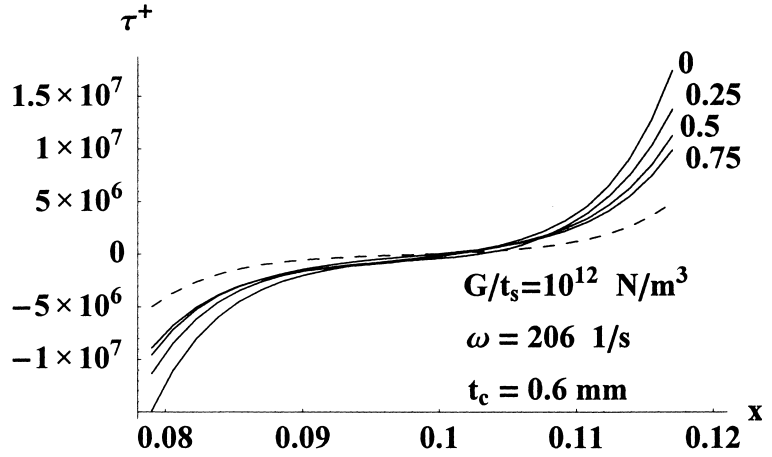

Fig. 13. Shear stress distribution in the upper bonding layer (no delamination) at $\omega = 206\ s^{-1}$.

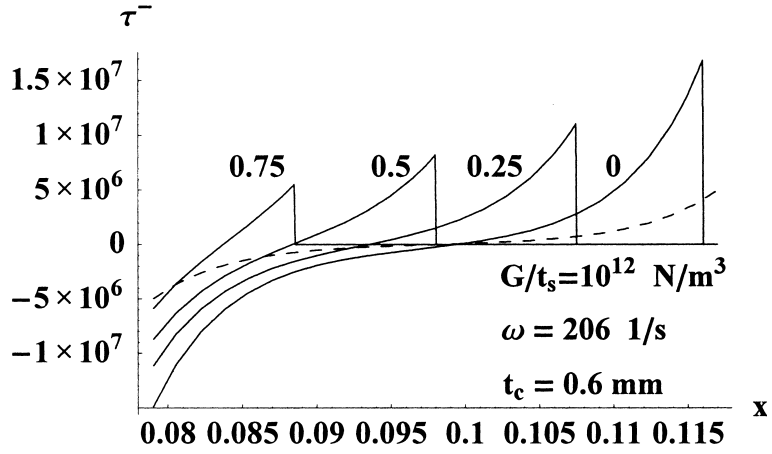

Fig. 14. Shear stress distribution in the lower bonding layer (delamination) at $\omega = 206\ s^{-1}$.

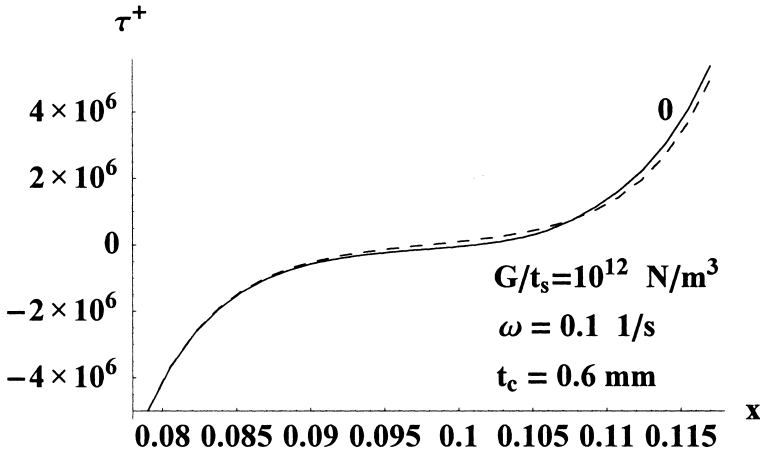

Fig. 15. Comparison of shear stress distributions in the upper bonding layer for low frequency excitation $\omega = 0.1\ s^{-1}$.

6. Conclusions

A dynamic model has been developed which is able to predict the response of a beam driven by the piezoelectric actuators glued to lower and upper beam surfaces. The actuators are driven by a pair of electrical fields with the same amplitude and in opposite phase. The actuators were used to excite steady-state harmonic vibrations in the beam. The results obtained from this analysis are compared with particular cases from past studies, which were based on the assumption of static coupling between the actuator and the beam. The numerical tests performed for the simply supported beam with surface bonded actuators show the influence of the delamination on the vibration characteristics. The increase of edge delamination decreases the magnitude of transfer functions between the applied voltage to the piezoactuators and the displacement of a fixed point of beam, and the shear stresses in the bonding layer, and the surface beam strains. The presented analytical model is a handy tool to the fast introductory obtaining of different dynamical characteristics of controlled structures with piezoactuators. The results can be applied to at least qualitative evaluation of the delamination harmful effect on piezoactuator coupling performance.

Acknowledgements

This study was supported by the State Committee for Scientific Research (Grant KBN – No 7T07A 04414).

References

Bailey, T., Hubbard, J.E., 1985. Distributed piezoelectric-polymer active vibration control of a cantilever beam. Journal of Guidance, Control and Dynamics 8, 605–611.

Bogdanovich, A., Rastogi, N., 1996. 3-D variational analysis of bonded composite plates, in: Proceedings of the ASME Aerospace Division. AD-52, ASME, 123–143.

Crawley, E.F., de Luis, J., 1987. Use of piezoelectric actuators as elements of intelligent structures. AIAA J 25, 1373–1385.

Jiang, W., Bao, G., 1996. Delamination induced buckling in orthotropic plate structures, in: Proceedings of the ASME Aerospace Division. AD-52, ASME, 31–38.

Jie, P., Hansen, C.H., Snyder, S.D., 1991. A Study of the Response of a Simply Supported Beam to Excitation by Piezoelectric Actuator. In: Rogers, C.A., Fuller, C.R. (Eds.), Recent Advances in Active Control of Sound and Vibration, Technomic Publishing, Lancaster-Basel, 39–49.

Mujumdar, P.M., Suryanarayan, S., 1988. Flexural vibrations of beams with delaminations. Journal of Sound and Vibrations 125, 441–461.

Newman, M.J., 1991. Distributed Active Vibration Controllers. In: Rogers, C.A., Fuller, C.R. (Eds.), Recent Advances in Active Control of Sound and Vibration, Technomic Publishing, Lancaster-Basel, 579–592.

Kim, S.J., Jones, J.D., 1992. Effects of piezo-actuator delamination on the performance of active noise and vibration control systems. DSC 38, Active Control of Noise and Vibration, ASME, 213–221.

Tylikowski, A., 1993. Stabilization of beam parametric vibrations. Journal of Theoretical and Applied Mechanics 31, 657–670.